Available online at www.sciencedirect.com
ScienceDirect
Trans. Nonferrous Met. Soc. China 22(2012) s110−s114
Transactions of Nonferrous Metals Society of China
www.tnmsc.cn

Sol−gel synthesis of Y_2O_3-doped ZnO thin films varistors and their electrical properties

XU Dong[1, 2, 3, 4, 5], JIANG Bin[1], JIAO Lei[1], CUI Feng-dan[1], XU Hong-xing[1], YANG Yong-tao[1, 6], YU Ren-hong[1, 6], CHENG Xiao-nong[1]

1. School of Material Science and Engineering, Jiangsu University, Zhenjiang 212013, China;
2. Key Laboratory of Semiconductor Materials Science, Institute of Semiconductors, Chinese Academy of Sciences, Beijing 100083, China;
3. State Key Laboratory of Electrical Insulation and Power Equipment, Xi'an Jiaotong University, Xi'an 710049, China;
4. State Key Laboratory of Electronic Thin Films and Integrated Devices, University of Electronic Science and Technology of China, Chengdu 610054, China;
5. Changzhou Engineering Research Institute of Jiangsu University, Changzhou 213000, China;
6. Changzhou Ming Errui Ceramics Co., Ltd., Changzhou 213102, China

Received 9 July 2012; accepted 19 August 2012

Abstract: Y_2O_3-doped ZnO−Bi_2O_3 thin films were fabricated on silicon substrates by sol–gel process and annealed in air at 750 °C for 1 h. Microstructure and electrical properties of ZnO thin films were investigated. XRD analysis shows that all peaks of ZnO thin films are well matched with hexagonal wurtzite structure of ZnO. SEM results present that the ZnO grain size decreases with the increase of dopant concentration, which means that rare earth doped can refine the grain size. The thickness of each layer is uniform and the value of thickness is about 80 nm. The nonlinear *V–I* characteristics with the leakage current of 0.46 μA, the threshold field of 110 V/mm and the nonlinear coefficient of 3.1 could be achieved when the films contain 0.2% (mole fraction) yttrium ion.
Key words: zinc oxide; Y_2O_3 varistor; film; sol-gel process; electrical properties; microstructure

1 Introduction

Zinc oxide, a semiconductor with wide band gap energy (−3.37 eV) is attracting attention for its potential applications as surge absorbers in electronic circuits, devices and electrical power systems to protect against dangerous over-voltage surges [1−3], because of its highly nonlinear current−voltage characteristics and a high energy absorption capability [4]. As a result, ZnO-based ceramic films are widely used to fabricate low voltage varistors [5].

Y_2O_3-doped ZnO varistor ceramics have attracted many researchers to investigate their microstructure and electrical characteristics. BERNIK [6,7] prepared Y_2O_3-doped ZnO–Bi_2O_3-based varistor ceramics. The results showed that the addition of Y_2O_3 resulted in the formation of a fine-grained Y_2O_3-containing phase along the grain boundaries of the ZnO grains which inhibits the grain growth. The threshold voltage (V_T) of the ceramics increased from 150 to 274 V/mm, the leakage current (I_L) also increased with the amount of Y_2O_3 added, and the nonlinear coefficient (α) was not influenced and remained at approximately 40 [6]. PARK et al [8] investigated Y_2O_3-doped Pr_6O_{11}−ZnO varistors and drew the conclusion that the threshold voltage ($V_{1.0\ mA}$), the nonlinear coefficient (α) and the average grain size increased with increasing the Y_2O_3 contents, whereas the dielectric constant (ε) decreased. The specimen with 4.0% (mole fraction) Y_2O_3 sintered at 1285 °C exhibited

Foundation item: Projects (BK2011243, BK2012156) supported by the Natural Science Foundation of Jiangsu Province, China; Project (EIPE11204) supported by the State Key Laboratory of Electrical Insulation and Power Equipment, China; Project (KF201104) supported by the State Key Laboratory of New Ceramic and Fine Processing, China; Project (KFJJ201105) supported by the Opening Project of State key Laboratory of Electronic Thin Films and Integrated Devices, China; Project (10KJD430002) supported by the Universities Natural Science Research Project of Jiangsu Province, China; Project (CJ20120058) supported by the Application Program for Basic Research of Changzhou, China; Project (11JDG084) supported by the Research Foundation of Jiangsu University, China
Corresponding author: XU Dong; Tel: +86-511-88797633; E-mail: frank@ujs.edu.cn

the highest nonlinearity, with a nonlinear coefficient (α) of 77, and the dielectric constant of 352 at 1 kHz. NAHM et al [9−13] researched the microstructure and electrical properties of Y_2O_3-doped ZnO−Pr_6O_{11}-based varistor ceramics in detail. Y_2O_3, as an inhibitor of grain growth, led to the decrease of the average grain size with the increase of its content. The varistor ceramics with Y_2O_3 content of 0.5% (mole fraction) sintered for 1 h exhibited the best performance in terms of *V–I* characteristics with 51.2 in the nonlinear coefficient, 1.3 μA in the leakage current.

An extensive literatures above indicate that among the rare earth oxides doped ZnO varistor ceramics, Y_2O_3 can largely inhibit the growth of ZnO grains, so that the threshold voltage of ZnO-based varistor ceramics are remarkably improved. But there is no study on the varistor properties of Y_2O_3-doped ZnO–Bi_2O_3-based thin films. It's significant for the further study of rare earth oxides doped ZnO thin films. Thus, it's essential to research Y_2O_3-doped ZnO thin films. In this work, the undoped and different concentrations of yttrium ion doped ZnO films were prepared by sol−gel process. The main goal is to investigate the effects of yttrium concentration on the microstructure and electrical properties with XRD and SEM analyses and *V–I* characteristics.

2 Experimental

Y_2O_3-doped ZnO−Bi_2O_3 thin films were fabricated on silicon substrates by sol−gel process. The steps, such as zinc acetate ($Zn(CH_3COO)_2{\cdot}2H_2O$), bismuth nitrate ($Bi(NO_3)_3{\cdot}2H_2O$) and manganese acetate ($Mn(CH_3COO)_2{\cdot}2H_2O$), were weighed according to the experimental scheme, which were dissolved in ethylalcohol with the addition of diethanolamine and glacial acetic acid, making the concentration of $Zn(CH_3COO)_2$ be 0.5 mol/L. In this way, making the final compositions of ZnO, Bi_2O_3 and MnO was in the relative molar ratio of 99:0.5:0.5 by adding the zinc acetate and the dopants. According to the different doping amounts of $Y(NO_3)_3$ (0, 0.1%, 0.2%, 0.3%, mole fraction), the samples were marked as QF0, QF1, QF2 and QF3, respectively. Finally, the samples were stirred at 60 °C for about 2 h to yield a clear, stable and homogeneous sol.

After aging for 48 h, the sol formed into a stable and homogeneous gel, the ZnO-based thin films were prepared by dip-coating at room temperature, dipping in the gel for 1 min. After previous steps, the films were heated at 400 °C in air for 10 min. After 8 layers have been deposited, the films were annealed at 750 °C in air for 1 h. At last, these films were allowed to cool inside the furnace.

The *V–I* characteristics of ZnO-based ceramic films were investigated by passing conductive adhesive tape on the surfaces of the films with a *V–I* source/measure unit (CJP CJ1001). The nominal varistor voltages (V_N) at 0.1 and 1.0 mA were measured, respectively, and the threshold voltage V_T (V/mm) was obtained according to $V_T=V_N/d$, where d is the thickness of the sample in mm. The nonlinear coefficient α ($\alpha=1/\lg(V_{1.0\ mA}/V_{0.1\ mA})$) was determined. The leakage current (I_L) was measured at $0.75V_N$ [2,3,14−24]. XRD of the ZnO thin films was measured by X-ray diffractometer (Rigaku D/max 2550 X-ray) with Cu K_α radiation. The microstructures of the ZnO films were observed by SEM (HITACHIs−4800).

3 Results and discussion

Figure 1 shows the XRD patterns of Y_2O_3-doped ZnO−Bi_2O_3 thin films. It could be seen that all diffraction peaks of ZnO thin films are well matched with hexagonal structure of ZnO. The diffraction peaks of Y_2O_3 are not found in Fig. 1. The most probable reason is that the amount of Y_2O_3 is too small to be found. That is to say, yttrium ions doped ZnO don't change the crystal structure, but instead of the crystal structure of Zn ions. This conclusion is also confirmed in the EDS analysis of ZnO−Bi_2O_3 thin films (not shown), and SAJID et al [25] prepared Co doped ZnO thin films by gel-combustion route and also proved this phenomenon.

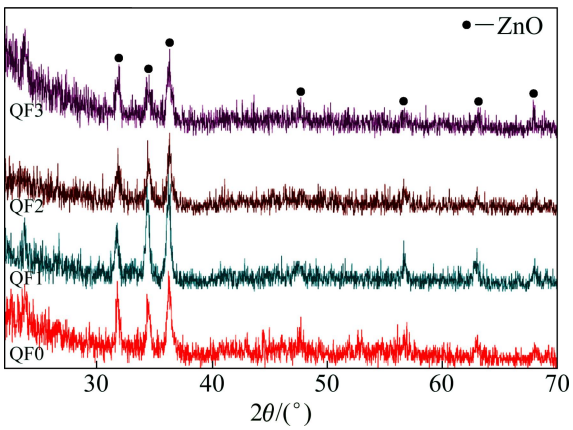

Fig. 1 XRD patterns of Y_2O_3-doped ZnO-Bi_2O_3 thin films

SEM microstructures of Y_2O_3-doped ZnO−Bi_2O_3 films are shown in Fig. 2. The average grain size of all micrographs is clearly below the micron. The grain size decreases with the dopant increasing, which means that rare earth doping can refine the grain size. This

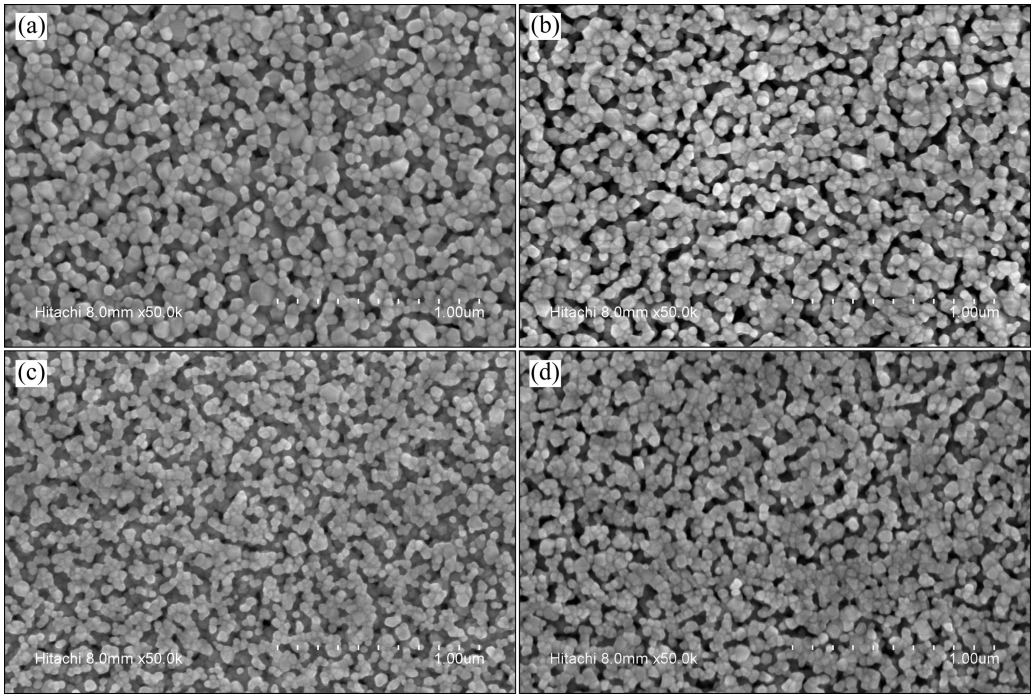

Fig. 2 SEM micrographs of Y_2O_3-doped ZnO−Bi_2O_3 thin films: (a) QF0; (b) QF1; (c) QF2; (d) QF3

phenomenon is the same as the researches of Refs [7,11]. On one hand, yttrium ion and zinc ion have different radii causing lattice distortion, which results in internal stress and destroys the order of the crystals. The internal stress increases with the dopant increasing, the lattice distortion becomes more serious. On the other hand, according to the crystal growth process, the crystal nucleation rate and growth rate are the two factors affecting the grain size. The radius of yttrium ion (0.102 nm) is larger than that of zinc ion, and a lot of yttrium ions cannot dissolve in ZnO. Thus, most of yttrium ions form new small grains on the grain boundaries, and promote the crystal nucleation rate. The pinning effect of these small grains effectively inhibits the grain growth. SEM micrographs of cross-sectional thickness of the investigated samples are shown in Fig. 3. Every layer can be clearly distinguished on the whole, and the thickness of each layer is about 80 nm. Among all layers, the thickness of the layers in the middle is uniform.

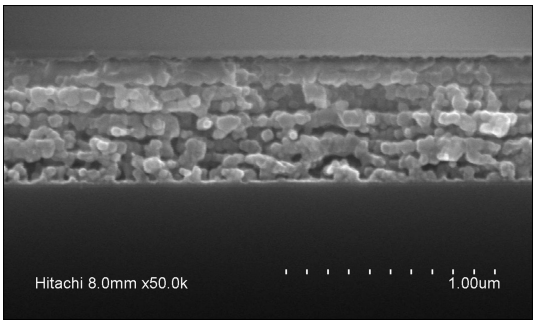

Fig. 3 SEM image of cross-sectional thickness of Y_2O_3-doped ZnO−Bi_2O_3 thin films

The leakage current I_L, threshold field V_T and nonlinear coefficient (α) of films are listed in Table 1. It is observed that the leakage current and threshold voltage firstly increase and then decrease and finally increase with the increase of Y_2O_3 content. The nonlinear coefficients of Y_2O_3-doped ZnO thin films samples have the opposite results that decrease at first, then increase and finally decrease, and reach a maximum value of 3.1 at 0.2% (mole fraction) yttrium ion. At the same time, the leakage current of the sample doped with 0.2% (mole fraction) yttrium ion is 0.46 mA, which is low relatively in the four samples.

Table 1 Leakage current, nonlinear coefficient and threshold field of films

Sample	I_L/mA	V_T/(V·mm^{-1})	α
QF0	0.38	128	2.4
QF1	0.49	186	2.3
QF2	0.46	110	3.1
QF3	0.51	159	2.1

4 Conclusions

1) The microstructure and electrical properties of ZnO thin films doped with different Y_2O_3 contents prepared by sol−gel process and annealed in air at 750 °C for 1 h were investigated.

2) XRD patterns show that all peaks of ZnO thin films are well matched with hexagonal structure of ZnO. SEM results indicate that the average grain sizes of all micrographs are clearly below the micron. With increasing Y_2O_3 content, the grain size of ZnO decreases, which means that the addition of rare earth can refine the grain size.

3) The thickness of each layer is about 80 nm and the thickness is uniform. When doped with 2.0% (mole fraction) yttrium ion, the leakage current of ZnO thin film is 0.46 mA while the threshold field is 110 V/mm and the nonlinear coefficient is 3.1.

References

[1] BERNIK S, ZUPANC P, KOLAR D. Influence of Bi_2O_3/TiO_2, Sb_2O_3 and Cr_2O_3 doping on low-voltage varistor ceramics [J]. Journal of the European Ceramic Society, 1999, 19(6−7): 709−713.

[2] XU D, SHI L Y, WU Z H, ZHONG Q D, WU X X. Microstructure and electrical properties of ZnO−Bi_2O_3-based varistor ceramics by different sintering processes [J]. Journal of the European Ceramic Society, 2009, 29(9): 1789−1794.

[3] XU D, CHENG X N, YAN X H, XU H X, SHI L Y. Sintering process as relevant parameter for Bi_2O_3 vaporization from ZnO−Bi_2O_3-based varistor ceramics [J]. Transactions of Nonferrous Metals Society of China, 2009, 19(6): 1526−1532.

[4] GUPTA T K. Application of zinc oxide varistors [J]. Journal of the American Ceramic Society, 1990, 73(7): 1817−1840.

[5] JIANG S L, ZHANG H B, HUANG Y Q, LIU M D, LIN R Z. Effect of annealing temperature of a novel sol−gel process on the electrical properties of low voltage ZnO-based ceramic films [J]. Materials Science and Engineering B, 2005, 117(3): 317−320.

[6] BERNIK S, MACEK S, AI B. Microstructural and electrical characteristics of Y_2O_3-doped ZnO−Bi_2O_3-based varistor ceramics [J]. Journal of the European Ceramic Society, 2001, 21(10−11): 1875−1878.

[7] BERNIK S, MACEK S, BUI A. The characteristics of ZnO-Bi_2O_3-based varistor ceramics doped with Y_2O_3 and varying amounts of Sb_2O_3 [J]. Journal of the European Ceramic Society, 2004, 24(6): 1195−1198.

[8] PARK J S, HAN Y H, CHOI K H. Effects of Y_2O_3 on the microstructure and electrical properties of Pr−ZnO varistors [J]. Journal of Materials Science: Materials in Electronics, 2005, 16(4): 215−219.

[9] NAHM C W. Effect of cooling rate on degradation characteristics of ZnO·Pr_6O_{11}·CoO·Cr_2O_3·Y_2O_3-based varistors [J]. Solid State Communications, 2004, 132(3−4): 213−218.

[10] NAHM C W. Microstructure and electrical properties of Y_2O_3-doped ZnO−Pr_6O_{11}-based varistor ceramics [J]. Materials Letters, 2003, 57(7): 1317−1321.

[11] NAHM C W, PARK C H. Microstructure, electrical properties, and degradation behavior of praseodymium oxides-based zinc oxide varistors doped with Y_2O_3 [J]. Journal of Materials Science, 2000, 35(12): 3037−3042.

[12] NAHM C W, SHIN B C. Effect of sintering time on electrical properties and stability against DC accelerated aging of Y_2O_3-doped ZnO−Pr_6O_{11}-based varistor ceramics [J]. Ceramics International, 2004, 30(1): 9−15.

[13] NAHM C W, SHIN B C. Highly stable nonlinear properties of ZnO−Pr_6O_{11}−CoO−Cr_2O_3−Y_2O_3-based varistor ceramics [J]. Materials Letters, 2003, 57(7): 1322−1326.

[14] XU D, ZHANG C, CHENG X N, FAN Y E, YANG T, YUAN H M. Dielectric properties of Zn-doped CCTO ceramics by sol-gel method [J]. Advanced Materials Research, 2011, 197−198: 302−305.

[15] XU D, CHENG X N, ZHAO G P, YANG J, SHI L Y. Microstructure and electrical properties of Sc_2O_3-doped ZnO−Bi_2O_3-based varistor ceramics [J]. Ceramics International, 2011, 37(3): 701−706.

[16] XU D, CHENG X N, YUAN H M, YANG J, LIN Y H. Microstructure and electrical properties of $Y(NO_3)_3·6H_2O$-doped ZnO−Bi_2O_3-based varistor ceramics [J]. Journal of Alloys and Compounds, 2011, 509(38): 9312−9317.

[17] WU Z H, FANG J H, XU D, ZHONG Q D, SHI L Y. Effect of SiO_2 addition on the microstructure and electrical properties of ZnO-based varistors [J]. International Journal of Minerals, Metallurgy and Materials, 2010, 17(1): 86−91.

[18] XU D, SHI X F, CHENG X N, YANG J, FAN Y E, YUAN H M, SHI L Y. Microstructure and electrical properties of Lu_2O_3-doped ZnO−Bi_2O_3-based varistor ceramics [J]. Transactions of Nonferrous Metals Society of China, 2010, 20(12): 2303−2308.

[19] XU D, CHENG X N, WANG M S, SHI L Y. Microstructure and electrical properties of La_2O_3-doped ZnO−Bi_2O_3-based varistor ceramics [J]. Advanced Materials Research, 2009, 79−82: 2007−2010.

[20] XU D, WANG B, LIN Y H, JIAO L, YUAN H M, ZHAO G P, CHENG X N. Influence of Lu_2O_3 on electrical and microstructural properties of $CaCu_3Ti_4O_{12}$ ceramics [J]. Physica B: Condensed Matter, 2012, 407(13): 2385−2389.

[21] XU D, ZHANG C, LIN Y H, JIAO L, YUAN H M, ZHAO G P, CHENG X N. Influence of zinc on electrical and microstructural properties of $CaCu_3Ti_4O_{12}$ ceramics prepared by sol−gel process [J]. Journal of Alloys and Compounds, 2012, 522: 157−161.

[22] XU D, TANG D M, LIN Y H, JIAO L, ZHAO G P, CHENG X N. Influence of Yb_2O_3 doping on microstructural and electrical properties of ZnO-Bi_2O_3-based varistor ceramics [J]. Journal of Central South University, 2012, 19(6): 1497−1502.

[23] XU D, TANG D M, JIAO L, YUAN H M, ZHAO G P, CHENG X N. Comparative characteristics of yttrium oxide and yttrium nitric acid doping on ZnO varistor ceramics [J]. Journal of Central South University, 2012, 19(8): 2094−2100.

[24] XU D, TANG D M, JIAO L, YUAN H M, ZHAO G P, CHENG X N. Effects of high-energy ball milling oxide-doped and varistor ceramic powder on ZnO varistor [J]. Transactions of Nonferrous Metals Society of China, 2012, 22(6): 1423−1431.

[25] ANSARI S A, NISAR A, FATMA B, KHAN W, NAQVI A H. Investigation on structural, optical and dielectric properties of Co doped ZnO nanoparticles synthesized by gel-combustion route [J]. Materials Science and Engineering B, 2012, 177(5): 428−435.

溶胶−凝胶法制备 Y_2O_3 掺杂 ZnO 压敏薄膜及其电性能

徐 东[1,2,3,4,5]，姜 斌[1]，焦 雷[1]，崔凤单[1]，徐红星[1]，杨永涛[1,6]，于仁红[1,6]，程晓农[1]

1. 江苏大学 材料科学与工程学院，镇江 212013；
2. 中国科学院半导体研究所 半导体材料科学重点实验室，北京 100083；
3. 西安交通大学 电力设备电气绝缘国家重点实验室，西安 710049；
4. 电子科技大学 电子薄膜与集成器件国家重点实验室，成都 610054；
5. 常州江苏大学工程技术研究院，常州 213000;
6. 常州明尔瑞陶瓷有限公司，常州 213102

摘 要：研究溶胶−凝胶法制备不同浓度 Y_2O_3 掺杂对 ZnO−Bi_2O_3 压敏薄膜微观结构和电性能的影响。研究结果表明：Y_2O_3 掺杂 ZnO 薄膜在 750°C 空气气氛下退火 1 h，ZnO 薄膜的特征峰与 ZnO 的六方纤锌矿结构相匹配；ZnO 晶粒直径随着掺杂量的增加而减小，Y_2O_3 稀土掺杂氧化锌晶粒细化；薄膜厚度均匀且每一层厚度约 80 nm。研究结果还表明：当 Y^{3+}掺杂浓度为 0.2%(摩尔分数)时，ZnO 薄膜的非线性伏安特性最好，其漏电流为 0.46 mA，电位梯度为 110 V/mm，非线性系数为 3.1。

关键词：氧化锌；Y_2O_3 压敏；薄膜；溶胶−凝胶法；电性能；显微组织

(Edited by DENG Lü-xiang)